

Received September 18, 2019, accepted October 7, 2019, date of publication October 14, 2019, date of current version October 25, 2019.

Digital Object Identifier 10.1109/ACCESS.2019.2947290

# A Comparative Experimental Analysis of Channel Access Protocols in Vehicular Networks

MOHAMED A. ABD EL-GAWAD<sup>1,2</sup>, MAHMOUD ELSHARIEF<sup>1,3</sup>,  
AND HYUNGWON KIM<sup>1</sup>, (Member, IEEE)

<sup>1</sup>Electronics Engineering Department, Chungbuk National University, Cheongju 28644, South Korea

<sup>2</sup>National Telecommunication Institute, Cairo 11768, Egypt

<sup>3</sup>Electrical Engineering Department, Al-Azhar University, Cairo 11651, Egypt

Corresponding Author: HyungWon Kim (hwkim@cbnu.ac.kr)

This work was supported in part by the Center for Integrated Smart Sensors through the Ministry of Science, ICT and Future Planning as the Global Frontier Project, South Korea, under Grant CISS-2019, in part by the Competency Development Program for Industry Specialists under the HRD Program for Intelligent Semiconductor Industry, Korean Ministry of Trade, Industry and Energy (MOTIE), through the Korea Institute for Advancement of Technology (KIAT) under Grant N0001883, and in part by the Korea Institute for Advancement of Technology (KIAT) through the Korean Government, Ministry of SMEs and Startups (MSS), under Grant S2755555.

**ABSTRACT** The deployment of vehicular networks is considered crucial for traffic safety of future vehicles. Thus, researchers are making extensive efforts to improve the performance of the IEEE802.11p standard. Many researchers have proposed various MAC protocols to mitigate the chronic problems of the IEEE802.11p – for example, the unreliable transmission of safety-related messages. However, most of the previous evaluations of the reliability problem have been done either via mathematical analysis or simulations. In this paper, we conducted actual experiments and analyzed the performance of two MAC protocols: IEEE802.11p and HCMAC, a hybrid MAC protocol recently reported. Using commercial V2X devices, we measured the performance in terms of received signal strength indicator (RSSI), packet delivery ratio (PDR), and packet inter-reception time (PIR). We tested the connectivity performance under various mobility scenarios. In addition, this paper investigates the impact of collisions on the overall performance. For a range of collision levels, an extensive set of experiments demonstrate that HCMAC outperforms the MAC of IEEE802.11p in terms of PDR and PIR up to 88% and 47%, respectively.

**INDEX TERMS** VANET, IEEE802.11p, HCMAC, Coda wireless, field testing.

## I. INTRODUCTION

Vehicular communication, often called vehicle-to-everything (V2X) communication, is among the main pillars for the imminent era of intelligent transportation systems (e.g., autonomous vehicles). Among many other benefits, V2X can improve road safety, reduce traffic congestion, and facilitate daily commute by exchanging real-time information between vehicles. For instance, vehicular communications can mitigate or eliminate human errors, which are reportedly responsible for over 80% of road accidents leading to 1.25 million fatalities worldwide in 2017 [1], [2].

V2X enables safety applications like left turn assist, intersection management assist, and lane change warning [3], which are aimed at mitigating human errors and improving safety conditions. Onboard applications rely on the beaconing mechanism, through which vehicles become aware

of the status of the neighboring vehicles. Each vehicle periodically broadcasts a message (i.e., beacon<sup>1</sup> message) containing the positional and kinematic information. The successful realization of safety applications requires a reliable and fast exchange of such beacon messages among neighboring vehicles, which presents a hard challenge to the underlying communication technology.

At the time of writing, there are two primary V2X technologies in the research and industry communities: IEEE 802.11p based V2X and 3GPP based cellular-V2X (C-V2X). The IEEE 802.11p [4] standard is an extension of the IEEE 802.11a Wi-Fi protocol with an enhancement of the quality to meet the vehicular communications goals. IEEE 802.11p's multiple access mechanism (Carrier Sense Multiple Access) cannot offer reliable broadcast. It also suffers from the hidden

The associate editor coordinating the review of this manuscript and approving it for publication was Maurice J. Khabbaz<sup>1</sup>.

<sup>1</sup>DSRC standard defines such a beacon message as a Basic Safety Message (BSM). Hereafter, the terms “beacon” and “BSM” are interchangeably used.

node problem. Therefore, on top of the physical layer of IEEE802.11p, many researchers have proposed other MAC protocols that offer a reliable broadcast service and solve the problem of hidden nodes. Some of these MAC protocols employ time division multiple access (TDMA) [5]–[8], and others introduce a hybrid mechanism by combining CSMA and TDMA [8]. Recently, 3GPP released C-V2X (Rel. 14), that is an extension of LTE Rel. 12's device-to-device (D2D) communications. C-V2X allows vehicles to communicate either through the network or in an ad-hoc fashion [9]. Self-organizing TDMA is also proposed as a low latency solution for the direct communication of C-V2X [10]. While it is not clear until now which technology will win the V2X market, there is a trend to formulate a global V2X platform that utilizes both technologies to adopt the advantages of both [11]. IEEE 802.11p is considered ahead of 3GPP C-V2X in the market since its state of standard and commercial readiness is more mature. This motivates us to conduct actual experiments and analyze the performance issues of IEEE802.11p-based V2X. In the literature, there are several works that have studied beaconing<sup>2</sup> performance only via either mathematical analysis or simulations [12]–[24]. On the other hand, there are very few reports on thorough experiments and performance analysis conducted using commercial IEEE802.11p V2X devices to our best knowledge—see section II.

In this paper, we conduct field experiments to assess the beaconing performance of IEEE802.11p in a real field environment. We show the impact of mobility on performance by testing vehicular communications in different mobility scenarios. We also illustrate how packet collisions impact the performance, especially in the dense networks. In our testing, we evaluate the performance using three important indicators; received signal strength indicator (RSSI), packet delivery ratio (PDR), and packet inter-reception time (PIR). In addition to the IEEE802.11p evaluation, this paper presents and evaluates the performance of HCMAC, a hybrid MAC protocol that combines TDMA and CSMA for V2X channel allocation. In [8], we show via mathematical analysis that the hybrid channel access mechanism of HCMAC can reduce the probability of collision. For the extended work presented in this paper, we implemented HCMAC on the commercial V2X devices and measured its performance in comparison with IEEE 802.11p. To the best of our knowledge, this is the first study that reports actual measurement for the performance of a hybrid MAC protocol like HCMAC. The experimental result section shows that HCMAC outperforms IEEE 802.11p in terms of PDR and PIR since HCMAC has the ability to avoid hidden collisions.

In summary, our contributions are as follows:

- Analyzing the beaconing performance of IEEE802.11p via conducting field testing with several mobility scenarios.

- Implementing the HCMAC protocol using commercial V2X devices.
- Demonstrating the actual performance improvement of HCMAC in comparison with IEEE802.11p measured from real field testing with various mobility scenarios.
- Investigating the influence of collisions on the beaconing performance of both protocols.

The remainder of this paper is organized as follows. Section II discusses related work, while Section III introduces the basic idea of HCMAC and explains its implementation. The details of measurement scenarios are presented in Section IV. In Section V, experimental results are presented, while the conclusions are given in Section VI.

## II. RELATED WORK

As mentioned earlier, due to the limited availability and high cost of the commercial V2X devices, the papers that reported beaconing performance in vehicular networks have only used either mathematical analysis or simulations. For instance, the authors of [12] analyzed the impact of vehicle density, message frequency, dissemination distance, and transmission range on beaconing performance of IEEE802.11p using only mathematical analysis. In [13], based on a thorough analysis, the authors designed a transmission range adaptation mechanism to mitigate the effect of the hidden node interference. Instead of employing a fixed contention window, [14] modeled the backoff process under unsaturated traffic conditions and proposed an adaptive contention window mechanism that can reduce the beacon collision probability. In [15], the authors developed an optimization problem to find the optimal beacon frequency by maximizing a utility function that considers the safety messages reliability. The authors in [16] analyzed the transmission success probability (TSP) of IEEE802.11p and expressed the distribution of TSP percentiles across the network. The authors solved an optimization problem to maximize the throughput by choosing the optimal transmission data rate. In [17], the authors modeled, with the aid of stochastic geometry, the periodic broadcast transmission with geolocation-based access (GLOC) for LTE-V2X networks. The authors analyzed the transmission success probability and energy efficiency. The authors in [18], improved the transmission reliability of LTE-V2X safety messages by applying a collision avoidance mechanism for both schedule assignment (SA) and data packets. The authors showed the enhanced performance in terms of packet reception ratio. In [19], the authors optimized the resource allocation in LTE-V2X networks, considering different sizes of periodic broadcast packets. The authors investigated the impact of some transmission parameters on the number of vehicles that can be simultaneously scheduled.

Several simulation studies evaluated the IEEE 802.11p performance [20]–[24]. In [20], the authors investigated the beaconing performance using NS-2 simulator under realistic mobility models in terms of latency, packet loss ratio (PLR), and throughput. They showed the effect of vehicle speed and

<sup>2</sup>This paper only focuses on evaluating the performance of BSM broadcasting over the control channel.

packet size on the network performance. In [23], the authors analyzed how the shadowing effect caused by surrounding vehicles and buildings affect the beacon dissemination performance. The provided simulation results show that there is no specific beacon interval that can fit all scenarios under the shadowing effect. Therefore, [23] proposed an adaptive beaconing algorithm that can reduce the performance loss due to the shadowing. The authors in [24], showed that applying network-coding mechanisms for broadcast packets can increase bandwidth utilization and reduce delivery time.

Some field experiments were conducted in [25]–[30]. In [25], the authors conducted their experiments using two laptops equipped with IEEE 802.11p cards instead of commercial IEEE 802.11p devices. The authors implemented their customized application over the traditional TCP/IP stack, so it periodically transmits fixed size UDP datagrams as a replacement of beacon messages. As an evaluation parameter, the authors measured the association time that represents the required time for a device to send a message and receive an acknowledgment. They obtained an association time of around 1.035 seconds which is too long to be employed for V2X network. This is because their packet transmission through TCP/IP stack incurs additional processing delays (e.g., sending an ARP packet to resolve the MAC address of the destination laptop). Wireless access in vehicular environments (WAVE) standard defines a new transport protocol called a wave short message protocol (WSMP-IEEE1609) which directly transfers beacon messages without going through the traditional processing like TCP/IP stack. Therefore, the emulation of beacon messages in [25] using UDP datagrams is not accurate enough to evaluate beaconing performance. In the study of [25], the authors also tested the transmission performance between a moving vehicle and a stationary one. The authors analyzed the transmission performance for vehicle speed of range 20 – 60 km/h and packet size of range 150 - 1460 bytes. They showed that a UDP packet of 500 bytes gives the best performance for all tested metrics.

In contrast to other studies, the authors of [26] introduced a new performance metric: PIR (i.e., the time difference between two successive beacon receptions). They showed the importance of PIR to analyze the time and frequency of blackouts (i.e., the time interval during which no beacon is received) that can directly affect safety application performance. The authors measured the PIR of beacon transmission between two moving vehicles using IEEE 802.11p compliant interfaces. They also illustrated that non-line of sight (NLOS) conditions severely degrade beaconing performance. The authors finally showed that applying simple multi-hop beaconing techniques can decrease the blackout frequency and, hence, improve the overall performance.

The authors in [27] measured the performance at an intersection where vehicles approaching from different directions exchange BSM messages. Via a road-side unit (RSU), the authors proposed relay mechanisms that retransmit some of the vehicles' BSMs to improve the broadcast reliability,

especially for NLOS communications. In [28], the authors evaluated the performance of the physical layer of IEEE 802.11p via MATLAB-based simulations. They measured the impact of signal to noise ratio (SNR) on bit error rate (BER) for all possible modulation schemes. They also investigated the effect of mobility on transmission quality. In addition, the authors conducted a field test using real IEEE 802.11p communication devices and performed an agreement between the simulation and experimental results. From their study, they found that high data rates (e.g., 18 and 24 Mbps) are not suitable for long-range communications (>200m). Moreover, they reported that moving vehicles with a relative speed of 220 km/h can substantially increase the PLR. In [29], the authors calibrated the existing path loss models (e.g., ITU-R P.1411) based on their measurements that they obtained for suburban and urban scenarios. The conducted experiments considered distance, small-scale fading, mobility effect, and traffic conditions. The authors in [30] conducted field testing to assess the performance of both DSRC and 4G-LTE in supporting different types of vehicular network applications. The obtained results showed that DSRC is more suitable for safety-related applications. On the other hand, 4G-LTE provides higher throughput and longer coverage range for multimedia applications.

In this paper, we employ commercial V2X devices that support both of IEEE802.11p and IEEE1609 protocols. We evaluate the beaconing performance of IEEE802.11p under different mobility scenarios. In addition, we analyze the impact of collision severity on the performance of beacon transmission. Moreover, we implement and test our cooperative MAC protocol, HCMAC [8] which combines TDMA and CSMA as a proposal of mitigating such experienced collisions.

### III. HCMAC PROTOCOL

This section describes HCMAC as an alternative MAC protocol to address the drawback of IEEE 802.11p standard. We first explain the basic ideas of HCMAC, and then provide the implementation methodology.

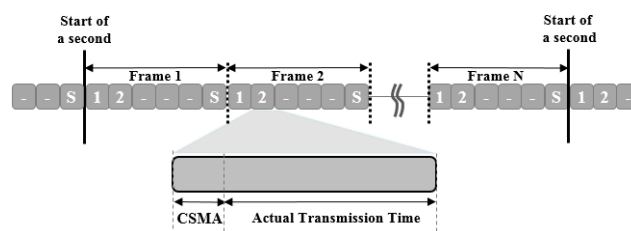


FIGURE 1. HCMAC time division structure.

#### A. HCMAC BASICS

HCMAC is a hybrid MAC protocol that we recently proposed for vehicular networks to operate over the physical layer of IEEE802.11p [8]. In HCMAC, the transmission time is divided into frames, and each frame is divided into a number

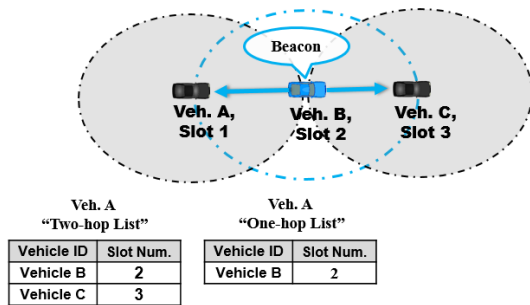


FIGURE 2. HCMAC cooperative slot acquisition.

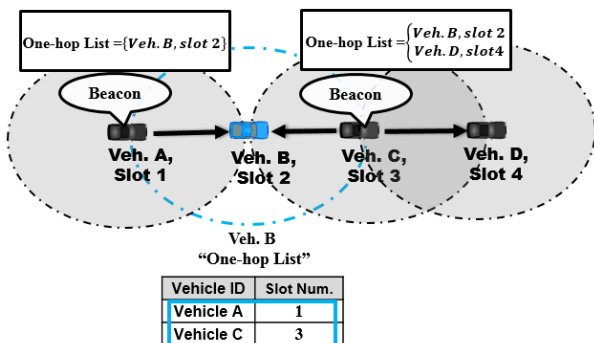


FIGURE 3. An example of how the attached one-hop lists act as implicit acknowledgments.

of fixed size slots as shown in Fig. 1. HCMAC introduces a fully distributed scheduling process where each vehicle can acquire a time slot by itself. In other words, there is no need for a central node or a base station to provide the scheduling.

To avoid the problems of duplicate slot acquisition and hidden-node collisions, each vehicle attaches to the beacon message a one-hop neighbor list (i.e., a list of neighboring vehicles that are located within the communication range). The one-hop list also conveys the acquired slots of the vehicles in the list. After receiving such information from all surrounding vehicles, the receiver vehicle constructs a list of all occupied slots for a two-hop communication range (see Fig. 2). Then, the receiver vehicle can acquire a free time slot and avoid the hidden terminal collisions. In other words, by exchanging the one-hop list through beacons, vehicles can identify the network topology, determine the time slots already occupied, and track any topology change that might occur due to vehicles' mobility. The attached one-hop list also represents a feedback mechanism that acts as implicit acknowledgments for the previous beacons received within the same TDMA frame. Fig. 3 explains an example of how vehicles employ the one-hop lists to acknowledge the reception of their beacon messages. In Fig. 3, suppose that vehicle B already sent a beacon message at slot 2 to its neighbors (vehicle A and vehicle C). Within the same TDMA frame, vehicle B expects a beacon message from vehicle A at slot 1 and another beacon from vehicle B at slot 3. If these beacons include vehicle B in the attached one-hop list, vehicle B

considers them as acknowledgments for the reception of its previous message. Otherwise, vehicle B concludes that its previous beacon has failed and then, it should select another slot to avoid any further collision.

Furthermore, HCMAC employs the CSMA contention mechanism within each time slot to reduce the probability of collisions that might happen due to a new vehicle joining the network or two networks merging (e.g., two or more vehicles that are located 3-hops away from each other might acquire the same time slot, and then they get closer up to a two-hop communication range). In HCMAC, whenever the vehicle detects an ongoing transmission, it stops transmitting over the acquired time slot and reacquires another free slot. In our previous work [8], we demonstrate via mathematical analysis that HCMAC can significantly reduce the collision probability compared to VeMAC [6] (a pure TDMA protocol).

In addition to our previous work of [8], this paper provides an extensive set of experimental results through a real implementation of HCMAC on commercial V2X devices and actual field test. It also exhibits a performance comparison with IEEE 802.11p.

### B. HCMAC IMPLEMENTATION

We implemented the functions of HCMAC protocol in a C program using the software development kit (SDK) and V2X device described in Section IV. The GPS time is used as a reference to provide the clock synchronization, which is necessary for all vehicles to calculate the correct time slots and frame boundaries. Therefore, the existing synchronization capabilities of V2X systems provide suitable conditions for TDMA protocols with fine time slots at no extra cost. We divide each second into 10 TDMA frames of 100 msec where each frame is further divided into 100 TDMA slots. Consequently, the TDMA slot width is 1 msec.

The GPS time periodically updates the system time of V2X devices every 200 msec [31]. This frequent time update guarantees that each V2X device keeps a perfect synchronization to the same reference time (i.e., the GPS time). Although each V2X device may have a different internal clock drift,<sup>3</sup> the periodic GPS time update can resolve such an issue and make all devices synchronized to each other. Once the V2X device receives the GPS signal, it can determine the TDMA slot and frame boundaries. In our implementation, we developed a function to adjust the system time and convert the UTC time to a TDMA map of time slots and frames as depicted in Fig.1. Based on the same obtained TDMA map, all V2X devices start the slot acquisition process by selecting a unique time slot, which is not occupied by any of their two-hop neighbors (to avoid the hidden terminal problem). Therefore, we modified the packet header to include the one-hop neighbor list in each transmitted beacon message. We also created a linked-list structure to store and merge

<sup>3</sup>The hardware clock of Cohda MK5 has an accuracy of 10 ppm, which can incur a maximum drift of 4 microseconds between two devices within the GPS update period (200 msec) [31].

the received one-hop neighbor lists that are received from neighboring vehicles. Another linked-list was created to store the constructed two-hop neighbor list. These linked-lists are continuously updated through time to reflect the dynamic change of network topology due to vehicles' mobility.

To identify the collisions, we implemented a function that tracks the reception of acknowledgments for each transmitted beacon message (as illustrated by the given example in Fig.3). Moreover, we used some CSMA-related primitive functions, which are already implemented in the V2X devices, to provide the HCMAC functionality of employing CSMA contention within each time slot. In particular, we use the functions that are developed for adjusting the contention window size and controlling the packet transmission.

#### IV. EXPERIMENT SETUP

In this section, we describe the V2X hardware devices used in the experiment, and the test scenarios.

**TABLE 1.** Specifications of MK5 OBUs/RSUs Cohda wireless modules.

| Parameter                    | Value                                   |
|------------------------------|---|
| Freq. Band                   | 5.9 GHz                                 |
| Channel Bandwidth            | 10 MHz                                  |
| TX power                     | -10 dBm to +23 dBm                      |
| Data Rates                   | 3, 4.5, 6, 12, 18, 24, 27 Mbps          |
| Receiver sensitivity @ 6Mbps | -97 dBm                                 |
| Standard Conformance         | IEEE 802.11p – 2012<br>IEEE 1609 - 2016 |
| GPS Accuracy                 | 2.5 meter                               |

##### A. HARDWARE CONFIGURATION

In the experiments, we used DSRC compliant devices, namely, the MK5 OBUs (On-Board Units) and MK5 RSUs (Road-Side Units) produced by Cohda Wireless [31]. These devices support the IEEE802.11p standard and the IEEE1609 protocols. Both OBUs and RSUs are equipped with a GPS receiver that provides time and position information. Table 1 summarizes the specifications of MK5 OBUs/RSUs. According to the US SAE standard [32], we configured the devices to use the control channel for BSM transmission (i.e., channel 178 at 5.9 GHz band). OBUs and RSUs periodically transmit BSM packets with a fixed frequency of 10 Hz, (i.e., the transmission interval is 100 msec). We configured the DSRC devices to transmit BSM packets with a data rate of 6 Mbps, a packet size of 200 bytes, and a TX power of 20 dBm.

##### B. MEASUREMENT SCENARIOS

We carried out all experiments in the testing track of Korea automotive technology institute (KATECH), Cheonan, South Korea (see Fig.4). This track was designed as a highway of 1 km length where all vehicles can communicate with line-of-sight (LOS) conditions. The OBU installed in each vehicle is controlled by a portable computer.



**FIGURE 4.** Aerial view of the testing track (Source: Google Maps).

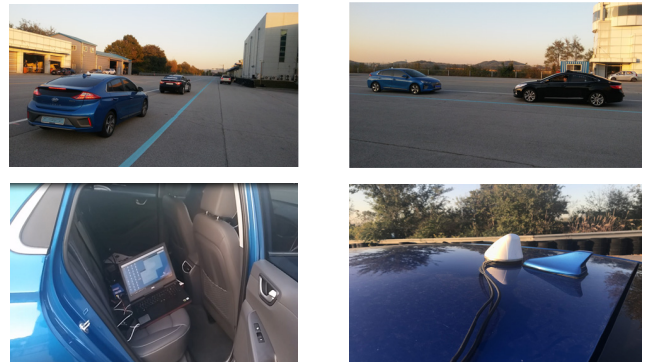


**FIGURE 5.** A general view of the conducted experiment.

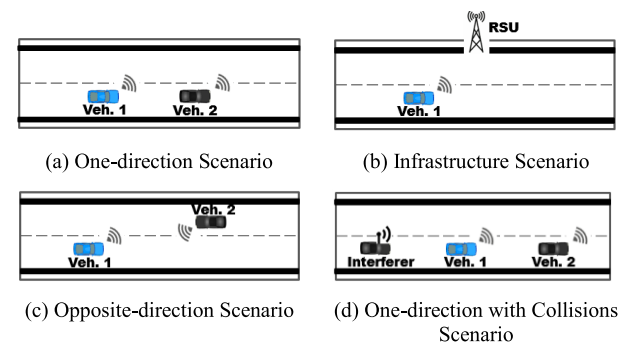


**FIGURE 6.** Measurements scenarios.

The antennas for DSRC and GPS are installed on the roof of the vehicle as shown in Fig. 5. For this experiment, we have developed a measurement software utility that records various performance metrics, including beacon reception counts, received RSSI, transmitter positions, and timestamps. We conducted the experiments in the following four scenarios; see Fig. 6.

**One-Direction Scenario:** two vehicles travel at the same speed with a fixed distance between the vehicles. Both vehicles start moving together from the start point to the end point of the track. The scenario is repeated with two different separation distances, and with 3 different speeds of 40 km/h, 70 km/h, and 90 km/h. We measured the average RSSI and calculated the PDR for each round.

**Infrastructure Scenario:** we installed an RSU at the halfway point of the track. While a vehicle travels at a constant speed along the track, it communicates with the RSU as shown in Fig. 6b. To analyze the mobility effect, this scenario

is repeated with 3 different speeds of 40 km/h, 70 km/h, and 90 km/h. We measured the RSSI and estimated the PDR for each speed configuration.

**Opposite-Direction Scenario:** this scenario assesses the performance under extreme mobility cases. It tests the link performance between two vehicles traveling in the opposite direction towards each other. In each run, the speed of both vehicles are set to 4 speeds of 40 km/h, 70 km/h, 90 km/h, and 100 km/h, which provides relative speeds of 80 km/h, 140 km/h, 180 km/h, and 200 km/h, respectively.

**One-Direction with Collisions Scenario:** this scenario is intended to measure the impact of packet collisions on the packet reception performance of the first scenario, i.e., One-direction scenario. In fact, generating a large number of packet collisions might have needed several interfering vehicles, which poses a serious challenge in vehicle operations and test cost. Therefore, we emulated network congestion in a range of severity, by adding one interfering vehicle as illustrated in Fig. 6(d). Via increasing the transmission frequency and packet size of the interfering vehicle's beacon packets, this scenario can change the channel congestion ratio (CCR) which is defined as the ratio of the time the channel is occupied over the entire period. Here, we only focused on hidden collisions. The reason is that; hidden collisions have a significant impact on packet loss while access collisions exhibit relatively small effect [33]. In Fig. 6(d), Vehicle2 and the interferer vehicle are hidden from each other (i.e., both vehicles are out of the communication range of each other). Unlike the previous scenarios, in this scenario, we have set the TX power to the minimum power of  $-10$  dBm, to intentionally create the situation of hidden nodes. Otherwise, the transmission with the default TX power of 20 dBm would have covered the entire track leaving no vehicles hidden from each other. In this scenario, the separation distance among vehicles is set to around 50 meters. We measured the communication performance from Vehicle2 to Vehicle1 and analyzed the effect of collisions on the reception performance of Vehicle1. We conducted this experiment for data rates of 6 Mbps and 12 Mbps.

## V. RESULTS

In this section, we first report the measurement results of end to end delay followed by the maximum connectivity range. We finally demonstrate the measurement obtained by the four test scenarios described above.

Since all measurements (except the last scenario) consider only one transmitter and one receiver (i.e., low channel load and no collisions), the results of HCSMAC are mostly equivalent to the results of IEEE802.11p. Therefore, the measured results up to Subsection F are the same for both protocols, so only one result is reported, while the remaining results exhibit a noticeable difference. The matching of obtained measurements (up to Subsection F) proves that HCSMAC achieves a similar connection performance in the absence of collisions at no extra cost.

### A. END-TO-END DELAY

This experiment reports the elapsed time for transmitting one beacon message between two vehicles. From the application's perspective, the measured time considers the transmission delay, propagation delay, and processing delay on both DSRC devices. We obtained an average delay of 1.00156 msec (the average is taken for 10000 packets), which is shorter than the delay reported in [25] (0.517 sec). As we mentioned in section II, the authors in [25] used an IEEE 802.11p platform that is not compliant to DSRC standard, and thus, their platform experienced extra latencies.

### B. MAXIMUM CONNECTIVITY RANGE

In this test, we measured the maximum distance between a transmitter and a receiver that maintains the packet delivery ratio (PDR) of at least 90 %. We observed a maximum distance of 800m for a PDR of 90%, when the vehicles are configured with a TX power of 20 dBm, a data rate of 6 Mbps, and a packet size of 200 bytes. In contrast, the authors of [28] had reported a distance of 700 meters, for a PDR of 60 %. It is difficult to make a direct comparison, however, since [28] used Arada LocoMate OBU [34] (a DSRC compliant OBU), and also [28] did not provide detailed specification such as the TX power. Our measurement reveals that with a data rate of 6 Mbps, the maximum range of 1000 meters as described in the specification can be obtained with an acceptable link quality in our LOS test environment.

TABLE 2. Average RSSI for the one-direction scenario.

| Speed (km/h) | Avg. Separation Distance (m) | Avg. RSSI (dBm) |
|--------------|------------------------------|-----------------|
| 40           | 35.62                        | -62.02          |
|              | 40.69                        | -64.64          |
| 70           | 36.01                        | -62.19          |
|              | 58.11                        | -64.15          |
| 90           | 35.69                        | -63.64          |
|              | 63.6                         | -65.41          |

### C. ONE DIRECTION SCENARIO RESULTS

Table 2 shows the average RSSI measured for various test configurations. For instance, the average RSSI is  $-64.15$  dBm for the test with a speed of 70 km/h and an average separation distance of 58.11m. Here, we calculated the average RSSI by considering only the good packets with no errors during the complete journey throughout the track. In addition, using the GPS in the DSRC device, we calculated the average distance between the vehicles throughout the test track. Table 3 demonstrates the PDR for the same test scenarios; In each test run throughout the track, we calculated the ratio of the actual reception count to the expected reception count as defined in Eq. 1. From the results of Table 3, we can observe that the PDR performance for the One-direction scenario slightly degrades as the speed increases. For example, for a separation distance of 35.6m, the PDR decreased

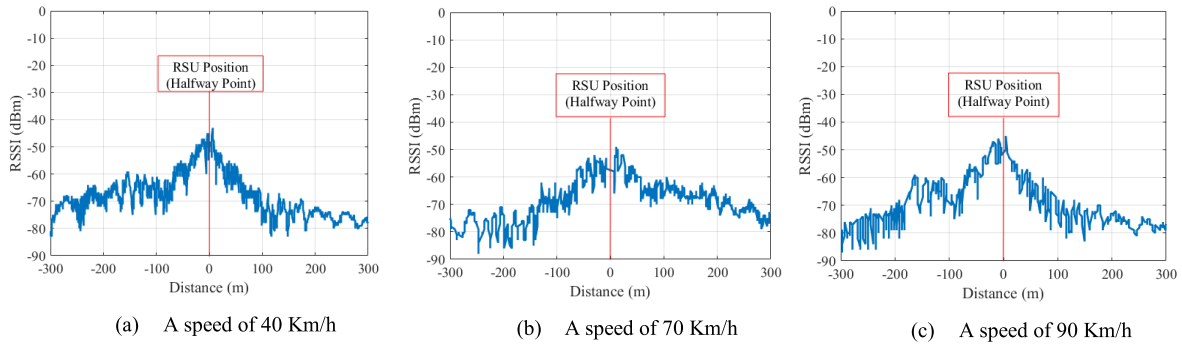


FIGURE 7. RSSI for the infrastructure scenario.

TABLE 3. PDR for the one-direction scenario.

| Speed (km/h) | Avg. Separation Distance (m) | PDR (%) |
|--------------|------------------------------|---------|
| 40           | 35.62                        | 99.2    |
|              | 40.69                        | 98.4    |
| 70           | 36.01                        | 97.3    |
|              | 58.11                        | 97.9    |
| 90           | 35.69                        | 95.6    |
|              | 63.6                         | 95.5    |

by 3.6% when the speed increased from 40 km/h to 90 km/h.

$$PDR = \frac{\text{The actual num. of receptions}}{\text{The expected num. of receptions}} \quad (1)$$

**D. INFRASTRUCTURE SCENARIO RESULTS**

While receiving from the RSU, the moving vehicle measured the RSSI of good beacon messages received with no errors. Fig. 7 shows the RSSI versus the distance for 3 different speed configurations. As the RSU is installed at the halfway point of the track, Fig 7 shows the RSSI measured for a separation distance in the range of [-300m to 300m]. As illustrated in Fig. 7, while the RSSI degrades as the distance increases, the trend of RSSI changes is nearly the same for all speed configurations.

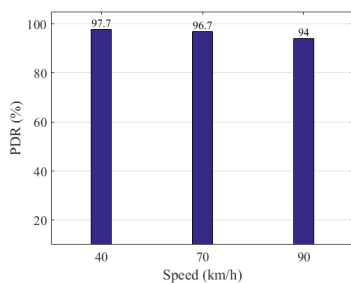


FIGURE 8. PDR for the infrastructure scenario.

Moreover, the moving vehicle measured the PDR for each run using Eq. 1. Fig. 8 reveals that the PDR degrades slightly as the speed increases. For example, the PDR decreased from 97.7% to 94%, when the speed increased from 40 km/h to 90 km/h. This small PDR loss is due to the Doppler

shift effect. Our observation differs from that of [28], which reported that the PDR decreased by around 10% for the same speed increment.

**E. OPPOSITE-DIRECTION SCENARIO RESULTS**

The objective of this experiment is to figure out how extreme mobility cases can affect beaconing performance. Fig. 9 illustrates the measured RSSI for relative speeds of 80 km/h, 140 km/h, 180 km/h, and 200 km/h. Fig. 9 shows that the RSSI mainly depends on the distance. For example, at a distance of 400m, the RSSI is around -80 dBm whatever the relative speed is. Furthermore, we calculated the PDR by applying Eq. 1, in Fig. 10, the obtained measurements show that driving with a relative speed of 200 km/h can achieve a PDR of 94% with a slight decrement (4%) than the 80 km/h case. Again, our finding differs from that of [28], which reported that the PDR decreased by around 13% for the same speed increment. We can conclude that with a data rate of 6 Mbps, the IEEE802.11p and HCMAC can achieve reliable beaconing performance even in intensive mobility cases.

TABLE 4. Average RSSI for the one-direction with collisions scenario.

| Avg. Separation Distance (m) | Avg. RSSI (dBm) |
|------------------------------|-----------------|
| 50                           | -89.1           |
| 60                           | -92             |
| 70                           | -94.4           |
| 80                           | -96.6           |

**F. ONE-DIRECTION WITH COLLISIONS SCENARIO RESULTS**

In the beginning, we show the measured average RSSI for the new TX power configuration (-10 dBm) to validate the hidden collision scenario as described in Section IV. Table 4 illustrates the average RSSI versus the distance between a transmitter and a receiver. For example, for a separation distance of 50m, the RSSI is around -89.1 dBm, while for a separation distance of 80m, the average RSSI decreases to around -96.6 dBm. In Fig. 6(d), the distance between the neighboring vehicles was 50m. Thus, Vehicle2 was 100m

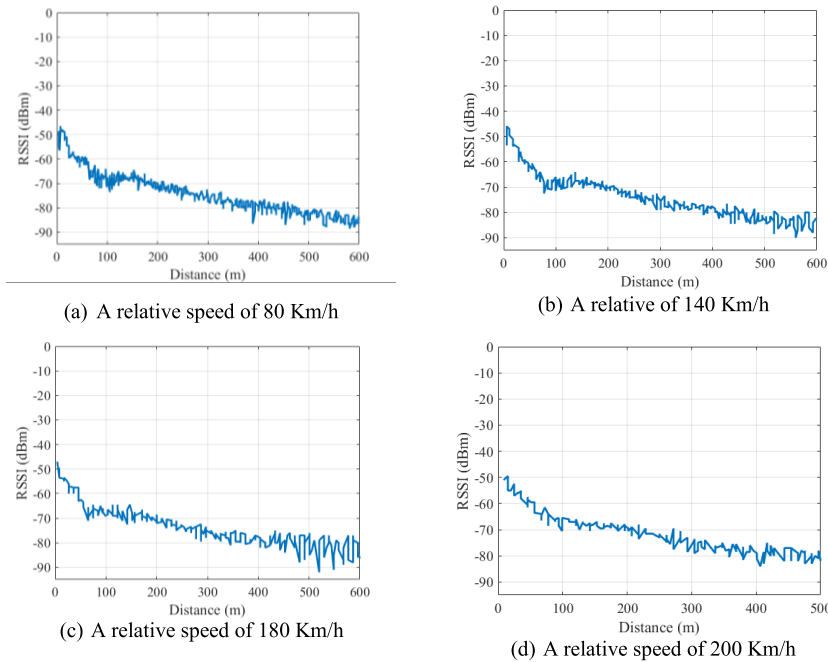


FIGURE 9. RSSI for the Opposite-Direction Scenario.

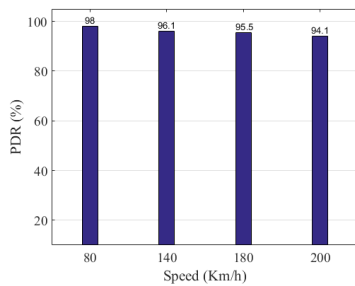


FIGURE 10. PDR for the Opposite-Direction Scenario.

away from the interferer vehicle. Keeping such distance made Vehicle2 and the interferer vehicle hidden from each other since they could not detect each other's signal. In other words, the RSSI of that signal was less than the receiver sensitivity ( $-97$  dBm). In order to evaluate various collision levels, we configured the interferer vehicle to transmit packets of various sizes and varying transmission intervals. In this scenario, we measured the PDR and PIR. From the measurements, we deduced the complementary cumulative distribution function (CCDF) of PIR that expresses the probability of having no received beacons (i.e., blackout) within a specific period of time. We first conducted this experiment without collisions to generate a performance baseline. Then, for different CCRs, we measured the beacons performance of both IEEE802.11p and HCMAC. In the previous scenarios, we showed that the speed has very little impact on performance. Thus, we only considered the stationary mobility case in this experiment.

Fig. 11 and Fig. 12 illustrate the impact of collisions on connection reliability. The X-axis of both figures

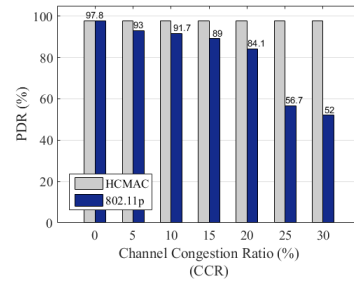


FIGURE 11. The packet delivery ratio (PDR) under different congestion levels (data rate = 6 Mbps).

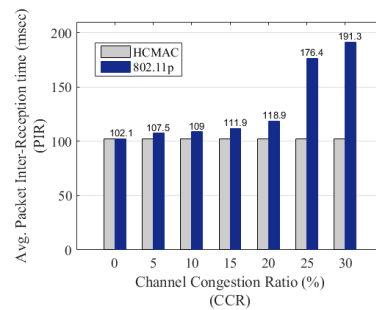
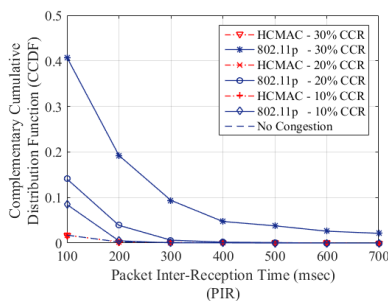


FIGURE 12. The Avg. Packet Inter-Reception time (PIR) under different congestion levels (data rate = 6 Mbps).

represents the CCR, which ranges from 0 to 30%. We controlled the CCR value, by configuring the transmission parameters (packet size and transmission interval) of the interferer vehicle. For example, a CCR of 10% corresponds to a packet size of 1500 bytes, and a transmission interval of 20 msec. Fig. 11 shows that increased collisions incur



large impact on PDR. For example, for a CCR of 15%, the PDR of IEEE802.11p is around 91.7%, while for a CCR of 30%, the PDR significantly decreases to 52%. Fig. 11 also demonstrates how the cooperative scheduling of HCMAC can mitigate the hidden collision effect and enhance beaconing performance. As shown in Fig. 11, HCMAC maintains the PDR at the maximum value regardless of the CCR level. For example, while HCMAC provides a constant PDR value of 97.8% even for a CCR of 30%, IEEE802.11p gives a PDR of only 52% for the same CCR. Fig. 12 illustrates the average PIR versus the CCR. We can observe that the average PIR of IEEE802.11p increases as the CCR level increases. For example, the PIR is around 111.9 msec at a CCR of 15%, while it increases to 191.3 msec at a CCR of 30%. In contrast, the PIR of HCMAC is a constant value of 102.15 msec for all CCR levels, which matches with the PDR results reported by Fig. 11.



**FIGURE 13.** The complementary cumulative distribution function (CCDF) of the packet inter-reception time (PIR) (data rate = 6 Mbps).

Since the average PIR cannot reveal the distribution of reception intervals, Fig. 13 compares the PIR performance over CCDF for IEEE802.11p and HCMAC. CCDF provides the probability that a node receives no beacon within a specific period of time. Fig. 13 illustrates the probability of the reception interval exceeding a target PIR (given by X-axis) for a range of CCR (given by different curves). For instance, for a CCR of 30%, the CCDF of IEEE802.11p is 0.4 for a target PIR of 100msec, which indicates that the probability of a node receiving the next beacon message in more than 100 msec is 40%. For the same CCR, CCDF of IEEE802.11p drops to 0.2 for a PIR of 200 msec, which means that the probability of the next reception in more than 200 msec is 20%. These results manifest how collisions can significantly degrade the V2X performance of IEEE802.11p. In contrast, HCMAC demonstrates a PIR performance of nearly the same level as the no-congestion case. For example, Fig. 13 shows that CCDF of HCMAC is as low as 0.02 for a PIR of 100msec. Such substantially shorter PIR performance is attributed to the fact that HCMAC can effectively alleviate the hidden-node collision problem.

Fig. 14 and Fig. 15 show the measured PDR and PIR using a data rate of 12 Mbps instead of 6 Mbps. The 12 Mbps cases show performance very similar to the 6 Mbps case shown in Fig. 11 and Fig. 12. This is due to the fact that the receiver is

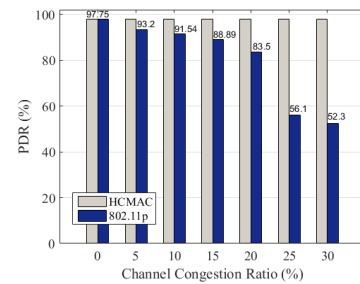


**FIGURE 14.** The packet delivery ratio (PDR) under different congestion levels (data rate = 12 Mbps).

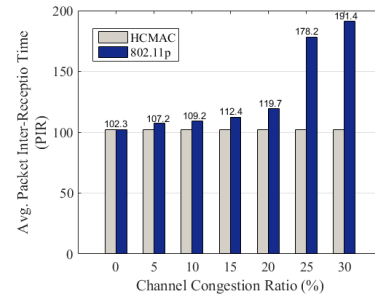


**FIGURE 15.** The packet delivery ratio (PDR) for the under different congestion levels (data rate = 12 Mbps).

not far from the transmitter (50 meters), and thus the receiver vehicle still exhibits the same performance as in the 6 Mbps case under various congestion scenarios.

From all the measurement results, we conclude that the collision is the dominant cause of performance degradation. Moreover, our experiments reveal that a cooperative scheduling mechanism like HCMAC can be an effective solution to substantially improving the performance and offering highly reliable beacon transmission even under heavy data traffic conditions.

## VI. CONCLUSION

This paper provided an experimental analysis for two MAC protocols: IEEE802.11p and HCMAC – the latter is an existing hybrid MAC protocol. Using commercial DSRC compliant devices, we implemented the HCMAC protocol on top of the IEEE802.11p physical layer. We then assessed the performance of beaconing messages (periodic safety packets) for IEEE802.11p and HCMAC, respectively, over various highway scenarios. We evaluated the performance in terms of RSSI, PDR, and PIR. The measurement exhibited that the mobility of the vehicles has little impact on connection performance. We also showed that packet collisions significantly degrade the beaconing performance. The experiments with various test scenarios showed that HCMAC outperforms IEEE802.11p up to 88% and 47% in PDR and PIR, respectively. Hence, IEEE802.11p can offer a reliable transmission only in the absence of collisions. Therefore, a cooperative transmission scheduling like HCMAC is a highly efficient solution to mitigating the collision problem and enhancing the overall performance.

## REFERENCES

- [1] The World Health Organization. *The World Health Report 2015—Reducing Risks, Promoting Healthy Life*. Accessed: Feb. 2, 2019. [Online]. Available: <http://www.who.int/whr/2002/chapter4/en/index7.html>
- [2] U.S. Department of Transportation, Bureau of Transportation Statistics. *National Transportation Statistics*. Accessed: Mar. 10, 2019. [Online]. Available: <https://www.bts.gov/topics/national-transportation-statistics>
- [3] The CAMP Vehicle Safety Communications Consortium consisting of BMW, “Vehicle safety communications project task 3 final report,” DaimlerChrysler, Ford, GM, Nissan, Toyota, and VW, CAMP Vehicle Saf. Commun. Consortium, Farmington Hills, MI, USA, Tech. Rep. DOT HS 809 859, Mar. 2005. [Online]. Available: <https://rosap.ntl.bts.gov/view/dot/3925>
- [4] *IEEE Standard for Wireless Access in Vehicular Environments (WAVE)—Networking Services*, IEEE Standard 1609.3-2016 (Revision of IEEE Standard 1609.3-2010), Apr. 2016, pp. 1–160.
- [5] W. Zhu, T. Hellmich, and B. Walke, “DCAP, a decentral channel access protocol: Performance analysis,” in *Proc. 41st IEEE Veh. Technol. Conf.*, May 1991, pp. 463–468.
- [6] H. A. Omar, W. Zhuang, and L. Li, “VeMAC: A TDMA-based MAC protocol for reliable broadcast in VANETs,” *IEEE Trans. Mobile Comput.*, vol. 12, no. 9, pp. 1724–1736, Jun. 2012.
- [7] M. Haddad, P. Muhlethaler, A. Laouiti, R. Zagrouba, and L. A. Saidane, “TDMA-based MAC protocols for vehicular ad hoc networks: A survey, qualitative analysis, and open research issues,” *IEEE Commun. Surveys Tuts.*, vol. 17, no. 4, pp. 2461–2492, 4th Quart., 2015.
- [8] M. A. A. El-Gawad, M. Elsharief, and H. Kim, “A cooperative V2X MAC protocol for vehicular networks,” *EURASIP J. Wireless Commun. Netw.*, vol. 2019, no. 1, p. 65, 2019.
- [9] *Vehicle to Vehicle (V2V) Services Based on LTE Sidelink; User Equipment (UE) Radio Transmission and Reception (Release 14)*, 3GPP TR 36.785, 2016.
- [10] L. Gallo and J. Härrä, “Self organizing TDMA over LTE sidelink,” Eurecom, Biot, France, Tech. Rep. RR-5105, 2017. [Online]. Available: <http://www.eurecom.fr/publication/5105>
- [11] Auto-Talks. *Accelerating Global V2X Deployment for Road Safety*. Accessed: Jan. 27, 2019. [Online]. Available: <https://www.auto-talks.com/wp-content/uploads/2018/09/Global-V2X-DSRC-and-C-V2X-whitepaper.pdf>
- [12] W. K. Wolterink, G. Heijenk, and H. van den Berg, “Analytically modelling the performance of piggybacking on beacons in VANETs,” in *Proc. 9th ACM Int. Workshop Veh. Inter-Netw., Syst., Appl.*, 2012, pp. 43–52.
- [13] Y. P. Fallah, C.-L. Huang, R. Sengupta, and H. Krishnan, “Analysis of information dissemination in vehicular ad-hoc networks with application to cooperative vehicle safety systems,” *IEEE Trans. Veh. Technol.*, vol. 60, no. 1, pp. 233–247, Oct. 2010.
- [14] Q. Yang, S. Xing, W. Xia, and L. Shen, “Modelling and performance analysis of dynamic contention window scheme for periodic broadcast in vehicular ad hoc networks,” *IET Commun.*, vol. 9, no. 11, pp. 1347–1354, 2015.
- [15] H. P. Luong, M. Panda, H. L. Vu, and B. Q. Vo, “Beacon rate optimization for vehicular safety applications in highway scenarios,” *IEEE Trans. Veh. Technol.*, vol. 67, no. 1, pp. 524–536, Aug. 2017.
- [16] M. A. A. El-Gawad, H. ElSawy, A. H. Sakr, and H. W. Kim, “Network-wide throughput optimization for highway vehicle-to-vehicle communications,” *Electronics*, vol. 8, no. 8, p. 830, 2019. doi: 10.3390/electronics8080830.
- [17] F. J. Martín-Vega, B. Soret, M. C. Aguayo-Torres, I. Z. Kovács, and G. Gómez, “Geolocation-based access for vehicular communications: Analysis and optimization via stochastic geometry,” *IEEE Trans. Veh. Technol.*, vol. 67, no. 4, pp. 3069–3084, Apr. 2018.
- [18] J. He, Z. Tang, Z. Fan, and J. Zhang, “Enhanced collision avoidance for distributed LTE vehicle to vehicle broadcast communications,” *IEEE Commun. Lett.*, vol. 22, no. 3, pp. 630–633, Mar. 2018.
- [19] A. Bazzi, A. Zanella, and B. M. Masini, “Optimizing the resource allocation of periodic messages with different sizes in LTE-V2V,” *IEEE Access*, vol. 7, pp. 43820–43830, 2019.
- [20] A. Jafari, S. Al-Khayatt, and A. Dogman, “Performance evaluation of IEEE 802.11p for vehicular communication networks,” in *Proc. 8th Int. Symp. Commun. Syst., Netw. Digit. Signal Process. (CSNDSP)*, Jul. 2012, pp. 1–8.
- [21] W. Alasmary and W. Zhuang, “Mobility impact in IEEE 802.11p infrastructureless vehicular networks,” *Ad Hoc Netw.*, vol. 10, no. 2, pp. 222–230, 2012.
- [22] S. Gräfling, P. Mähönen, and J. Riihijärvi, “Performance evaluation of IEEE 1609 WAVE and IEEE 802.11p for vehicular communications,” in *Proc. IEEE 2nd Int. Conf. Ubiquitous Future Netw. (ICUFN)*, Jun. 2010, pp. 344–348.
- [23] C. Sommer, S. Joerer, M. Segata, O. K. Tonguz, R. L. Cigno, and F. Dressler, “How shadowing hurts vehicular communications and how dynamic beaconing can help,” *IEEE Trans. Mobile Comput.*, vol. 14, no. 7, pp. 1411–1421, Oct. 2014.
- [24] G. G. M. N. Ali, M. Noor-A-Rahim, M. A. Rahman, S. K. Samantha, P. H. J. Chong, and Y. L. Guan, “Efficient real-time coding-assisted heterogeneous data access in vehicular networks,” *IEEE Internet Things J.*, vol. 5, no. 5, pp. 3499–3512, Oct. 2018.
- [25] F. A. Teixeira, V. F. e Silva, J. L. Leoni, D. F. Macedo, and J. M. Nogueira, “Vehicular networks using the IEEE 802.11p standard: An experimental analysis,” *Veh. Commun.*, vol. 1, no. 2, pp. 91–96, 2014.
- [26] M. E. Renda, G. Resta, P. Santi, F. Martelli, and A. Franchini, “IEEE 802.11p VANets: Experimental evaluation of packet inter-reception time,” *Comput. Commun.*, vol. 75, pp. 26–38, Feb. 2016.
- [27] N. Hieu, M. Noor-A-Rahim, Z. Liu, D. Jamaludin, and Y. Guan, “A semi-empirical performance study of two-hop DSRC message relaying at road intersections,” *Information*, vol. 9, p. 147, Jun. 2018. doi: 10.3390/info9060147.
- [28] A. Sassi, Y. Elhillali, and F. Charfi, “Evaluating experimental measurements of the IEEE 802.11p communication using ARADA LocoMate OBU device compared to the theoretical simulation results,” *Wireless Pers. Commun.*, vol. 97, no. 3, pp. 3861–3874, 2017.
- [29] L. I. Fang, C. Wei, J. Wang, S. Yishui, Y. Kun, X. Lida, Y. Junyi, and L. Changzhen, “Different traffic density connectivity probability analysis in VANETs with measured data at 5.9 GHz,” in *Proc. IEEE 16th Int. Conf. Intell. Transp. Syst. Telecommun. (ITST)*, Oct. 2018, pp. 1–7.
- [30] Z. Xu, X. Li, X. Zhao, M. H. Zhang, and Z. Wang, “DSRC versus 4G-LTE for connected vehicle applications: A study on field experiments of vehicular communication performance,” *J. Adv. Transp.*, vol. 2017, Aug. 2017, Art. no. 2750452.
- [31] *Cohda Wireless MK5 OBU & RSU*. Accessed: Feb. 4, 2019. [Online]. Available: <https://cohdawireless.com/solutions/hardware/>
- [32] *Dedicated Short Range Communications (DSRC) Message Set Dictionary*. Accessed: Oct. 20, 2018. [Online]. Available: [http://standards.sae.org/j2735\\_201603/](http://standards.sae.org/j2735_201603/)
- [33] S. Gonzalez and V. Ramos, “A simulation-based analysis of the loss process of broadcast packets in WAVE vehicular networks,” *Wireless Commun. Mobile Comput.*, vol. 2018, Oct. 2018, Art. no. 7430728. doi: 10.1155/2018/7430728.
- [34] Arada Syatems. *Locomate OBU*. Accessed: Jan. 3, 2019. [Online]. Available: <http://files.moonblink.com/Arada-Locomate-OBU.pdf>



**MOHAMED A. ABD EL-GAWAD** received the B.Sc. degree in electrical engineering from Assiut University, Assiut, Egypt, in 2006, and the M.Sc. degree in electrical engineering from the Arab Academy for Science and Technology, Cairo, Egypt, in 2013. He is currently pursuing the Ph.D. degree with the Department of Electrical and Computer Engineering, Chungbuk National University, South Korea. From 2008 to 2015, he was with the National Telecommunication Institute, Egypt,

where he conducted professional training as well as research on wireless communications. In 2016, he joined the MSIS Lab, Cheongju, South Korea, as a Student Researcher. His current research interests include wireless sensor networks and vehicular communications.



**MAHMOUD ELSHARIEF** received the B.S. degree in communications and electronics engineering from Al-Azhar University, Cairo, Egypt, in 2010, the M.S. degree in communications and electronics engineering from Ain Shams University, Cairo, in 2014. He is currently pursuing the Ph.D. degree with the Electronics Engineering Department, Chungbuk National University, Cheongju, South Korea. From 2012 to 2016, he was a Researcher and Teaching Assistant with the

Communications and Electronics Engineering Department, Al-Azhar University, Cairo. His current research interests focus the areas of wireless sensor networks and wireless vehicular communications.



**HYUNGWON KIM** (M'95) received the B.S. and M.S. degrees in electrical engineering from the Korea Advanced Institute of Science and Technology (KAIST), in 1991 and 1993, respectively, and the Ph.D. degree in electrical engineering and computer science from the University of Michigan, Ann Arbor, MI, USA, in 1999. In 1999, he joined Synopsys Inc., Mountain View, CA, USA, where he developed electronic design automation software. In 2001, he joined Broadcom Corporation, San Jose, CA, USA, where he developed various network chips, including a WiFi gateway router chip, a network processor for 3G, and 10gigabit ethernet chips. In 2005, he founded Xronet Corporation, a Korean-based wireless chip maker, where he was the CTO and CEO. He managed the company to a successfully developed and commercialize wireless baseband and RF chips and software, including WiMAX chips supporting IEEE802.16e and WiFi chips supporting IEEE802.11a/b/g/n. Since 2013, he has been with Chungbuk National University, Cheongju, South Korea, where he is currently an Associate Professor with the Department of Electronics Engineering. His current research interests focus the areas of sensor read-out circuits, touch screen controller SoC, wireless sensor networks, wireless vehicular communications, mixed signal SoC designs for low power sensors, and bio-medical sensors.